6562 *Biochemistry* **2009,** *48,* 6562–6570
DOI: 10.1021/bi900371p

BIOCHEMISTRY
including biophysical chemistry & molecular biology
Current Topic

Reaction Kinetics, Catalytic Mechanisms, Conformational Changes, and Inhibitor Design for Prenyltransferases

Po-Huang Liang*

Institute of Biological Chemistry, Academia Sinica, Taipei, Taiwan

Received March 5, 2009; Revised Manuscript Received June 16, 2009

ABSTRACT: Isoprenoids comprise a family of more than 55000 natural products with great structural variety derived from five-carbon isopentenyl diphosphate (IPP) and its isomer dimethylallyl diphosphate (DMAPP). Allylic diphosphates such as farnesyl diphosphate (FPP) synthesized from DMAPP and IPP serve as outlet points for a great variety of products. A group of prenyltransferases catalyzing chain elongation of FPP to designated lengths by consecutive condensation reactions with specific numbers of IPP are classified as *cis* and *trans* types according to the stereochemistry of the double bonds formed by IPP condensation. The complete kinetics of the multistep IPP condensation reactions by both types of enzymes has been determined using steady-state and pre-steady-state approaches. Because their crystal structures were determined in conjunction with biochemical studies, a more thorough understanding of their catalytic mechanisms, protein conformational changes, and product chain-length determination mechanisms has been gained recently. Since these prenyltransferases play important roles, potent inhibitors have been identified and their cocrystal structures have been determined for drug development. In this review, the current knowledge of these prenyltransferases that synthesize prenyl oligomers or polymers is summarized.

Isoprenoids make up an important family of natural products built on the five-carbon isopentenyl diphosphate (IPP)[1] (*1*, *2*). More than 55000 naturally occurring isoprenoid molecules have been discovered, with a large number of new structures reported each year (*3*). IPP is synthesized from three molecules of acetyl coenzyme A through the classic mevalonate pathway, and in some bacteria and plants from a nonclassic methylerythritol phosphate pathway (*4*, *5*). IPP is then converted to its isomer dimethylallyl diphosphate (DMAPP) by IPP:DMAPP isomerase (*6*). By condensation of DMAPP with one to three molecules of IPP, C_{10}-geranyl diphosphate (GPP), C_{15}-farnesyl diphosphate (FPP), and C_{20}-genanylgeranyl diphosphate (GGPP) are synthesized by the respective synthases, GPPs, FPPs, and GGPPs. These short-chain-length products serve as precursors leading to a variety of natural isoprenoid products such as sterols, carotenoids, dolichols, ubiquinones, and prenylated proteins (as shown in Figure 1A for some of their biosyntheses) found in all organisms, functioning as hormones, visual pigments, constituents of membranes, and components of signal transduction (*7*).

*To whom correspondence should be addressed. Telephone: 886-2-2785-5696, ext. 6070. Fax: 886-2-2788-9759. E-mail: phliang@gate.sinica.edu.tw.

[1]Abbreviations: IPP, isopentenyl diphosphate; DMAPP, dimethylallyl diphosphate; GPP, geranyl diphosphate; FPP, farnesyl diphosphate; GGPP, geranylgeranyl diphosphate; GPPs, geranyl diphosphate synthase; FPPs, farnesyl diphosphate synthase; GGPPs, geranylgeranyl diphosphate synthase; HexPPs, hexaprenyl diphosphate synthase; OPPs, octaprenyl diphosphate synthase; UPPs, undecaprenyl diphosphate synthase; DPPs, decaprenyl diphosphate synthase; PDB, Protein Data Bank.

FPP can be elongated to a variety of linear polyprenyl diphosphates via consecutive condensation reactions with specific numbers of IPP by a group of prenyltransferases (*8*−*10*). These enzymes are classified as *cis* and *trans* types according to the stereochemistry of double bonds from IPP condensation. *trans*-Prenyltransferases identified so far synthesize products with chain lengths from C_{10} to C_{50}. In terms of their biological functions, C_{15}-FPP and C_{20}-GGPP can be used as ligands for posttranslational modifications of signaling proteins such as Ras, Rab, nuclear lamins, trimeric G-protein γ subunits, protein kinases, and small Ras-related GTP-binding proteins for anchoring into the cell membrane for cell proliferation and differentiation (*11*). Therefore, FPPs and GGPPs serve as targets for cancers and bone resorption diseases such as osteoporosis (*12*). The C_{20} and C_{25} compounds by GGPPs and farnesylgeranyl diphosphate synthase, respectively, can be assembled into ether-linked lipids in thermophilic *archaea* (*13*). The products of C_{30} hexaprenyl diphosphate synthase (HexPPs), C_{35} heptaprenyl diphosphate synthase, C_{40} octaprenyl diphosphate synthase (OPPs), C_{45} solanesyl diphosphate synthase, and C_{50} decaprenyl diphosphate synthase form the side chains of ubiquinones in different species (*13*). Most short-chain prenyltransferases are active as homodimers (e.g., the GGPPs structure shown in the table of contents graphic), whereas homo- and heteromers (e.g., HexPPs) have been observed among the medium- and long-chain enzymes.

In contrast, *cis*-prenyltransferases catalyzing condensation of IPP produce larger products ($> C_{50}$) with the exception of a short-chain C_{15}-FPP catalyzed by a *cis*-type FPPs from *Mycobacterium*

 Published on Web 06/19/2009

tuberculosis (*14*). The medium-chain C_{55} product of the bacterial undecaprenyl diphosphate synthase (UPPs), a dimeric enzyme as shown in the table of contents graphic, serves as a lipid carrier in cell wall peptidoglycan biosynthesis (*15*). In that pathway, UPP undergoes dephosphorylation by phosphatases to undecaprenyl monophosphate and links with *N*-acetylmuramyl pentapeptide and *N*-acetylglucosamine to form lipid II that is then transported across the cell membrane via translocase and assembled together by transglycosylase and transpeptidase to form peptidoglycan (*16*). Its homologous dehydrodolichyl diphosphate synthases from eukaryotes such as yeast Srt1p and Rer2p and human *cis*-prenyltransferase are responsible for making $> C_{100}$ dolichols to mediate glycoprotein biosynthesis (*17*). In an extreme case, rubber prenyltransferase synthesizes natural rubber containing thousands of IPP units (*18*).

We mainly worked on the structural and mechanistic studies of the short-chain-length *trans*-GGPPs from *Saccharomyces cerevisiae* and the long-chain-length *trans*-OPPs from *Escherichia coli* as well as the *cis*-UPPs from *E. coli*. In this review, the current understanding of the reaction kinetics, catalytic mechanisms, conformational changes, and inhibitor design for these and other prenyltransferases is summarized.

REACTION KINETICS

The prenyltransferases catalyze multiple IPP condensation reactions, yielding linear prenyl oligomers or polymers. To determine whether each IPP condensation step proceeds with similar or different rates and what the rate-limiting step is, the reaction kinetics of *cis*-UPPs and *trans*-OPPs were examined by using the transient kinetic methods (i.e., rapid-quench and stopped-flow technologies). The reactions under the single-turnover condition, where the E concentration is higher than the FPP concentration, were stopped on a millisecond time scale using rapid-quench apparatus, and the intermediates with increased numbers of [^{14}C]IPP were analyzed by reverse-phase TLC (*19*, *20*). The time courses for chain-elongating intermediates deduced from TLC data were simulated with the kinetic simulation program (KinSim) to yield the rate constants for IPP condensation steps. The rate constants for five IPP condensation steps catalyzed by OPPs are similar, which are approximately 2 s^{-1} (Figure 1B), and those for eight IPP condensation steps catalyzed by UPPs are ~2.5 s^{-1} (Figure 1C). Furthermore, it was shown that 0.1% Triton X-100 increases the steady-state k_{cat} value of UPPs from 0.013 to 2.5 s^{-1}, indicating different rate-limiting steps for the UPPs reaction with and without detergent (*19*). In the absence of Triton, slow product release limits the UPPs steady-state rate, whereas the detergent facilitates the product release; thus, the rate-limiting step is shifted to IPP condensation which has a rate of 2.5 s^{-1} based on the single-turnover reaction. Slow product release as the rate-limiting step in the absence of detergent was confirmed by a burst kinetic profile for the UPP product formation versus time (*19*). It was also demonstrated by using a fluorescent FPP analogue as a competing agent in the stopped-flow experiments that UPP product release is slow and its rate matches the steady-state kinetic constant in the absence of detergent (*21*).

In contrast, no stimulating effect by Triton or any other tested detergents was found for the OPPs reaction (*20*). However, the kinetic constant measured under steady-state conditions is also significantly smaller than that obtained under the single-turnover condition, indicating that a step slower than IPP condensation limits the k_{cat} for the OPPs reaction.

Establishment of the IPP condensation kinetics by transient kinetic methods for *cis*- and *trans*-prenyltransferases provides a great advantage for kinetic characterization of these prenyltransferases and their mutants (*22*). The steady-state k_{cat} values can be measured with 0.1% Triton X-100 (a higher concentration can inhibit the enzyme activity) to reflect the rate constant of IPP condensation catalyzed by UPPs. The kinetic measurements also indicate similar activation energy for *cis* and *trans* types of IPP condensation reactions, although different catalytic strategies are used as illustrated below.

CATALYTIC MECHANISMS

Two possible mechanisms proposed for prenyltransferase reactions are (1) a sequential ionization−condensation−elimination mechanism in which the allylic substrate releases its diphosphate to form a carbocation intermediate, which is attacked by IPP, and a proton (H_R for the *trans* type) is removed from IPP C2 to form the adduct and (2) a concerted condensation−elimination mechanism in which ionization of the allylic substrate and condensation of IPP occur simultaneously (*23*). *trans*-type FPPs and OPPs have been shown to proceed through a sequential mechanism as shown in Figure 1B (*24*, *25*). In contrast, *cis*-type UPPs may utilize a concerted mechanism as shown in Figure 1C, which is consistent with the failure to trap the carbocation intermediate as farnesol under basic conditions from the FPP substrate in the presence of an IPP analogue, Br-IPP, to slow the condensation step (*25*). Under the same conditions, farnesol was trapped in the OPPs reaction. *cis*- and *trans*-prenyltransferases may utilize different strategies for catalysis, as suggested by the lack of sequence similarity (*26*, *27*). The known crystal structures show that *trans*-prenyltransferases use two conserved DDxxD motifs to coordinate Mg^{2+} ions for binding with the allylic substrate diphosphate group (*28*−*35*), whereas an Asp in the conserved P-loop of *cis*-type prenyltransferases (D26 in *E. coli* UPPs) plays the Mg^{2+}-chelating role (*36*−*40*).

On the basis of the crystal structure of *E. coli* FPPs complexed with the allylic substrate thiol analogue DMSPP and IPP (shown in the right panel of Figure 1B), DMSPP is bound to FPPs through a trinuclear Mg^{2+} cluster that is coordinated by three conserved Asp residues (*31*). Two Mg^{2+} ions each form six-membered ring chelated structures with two unesterified pyrophosphate oxygens, while the other Mg^{2+} ligates a single unesterified oxygen of the linking pyrophosphate. The carbocation from the allylic substrate is stabilized by electrostatic interactions with the released pyrophosphate and also through the main-chain carbonyl oxygen of Lys202 and the side-chain oxygens of Thr203 and Gln241. The homoallylic substrate IPP is bound in a positively charged pocket formed by Lys, Arg, and His residues. These interactions position the nucleophilic C3−C5 double bond of IPP 3.2 Å from the C1 atom of DMSPP. A nonmetal ligated pyrophosphate oxygen (ligated by conserved Arg116 and Lys258) is correctly positioned to abstract the IPP C2 H_R after the condensation reaction (see the left panel of Figure 1B for the mechanism).

On the other hand, on the basis of the crystal structures of *E. coli* UPPs in complex with FsPP (FPP thiol analogue) and IPP (shown in the right panel of Figure 1C), an Asp26-coordinated Mg^{2+} ion is bound to the diphosphate group of FsPP (*40*). When Asp26 is mutated to Ala, IPP diphosphate is bound to the Mg^{2+}, but Mg^{2+} is at a slightly different position based on the crystal structure. Thus, a Mg^{2+} transfer mechanism was proposed in

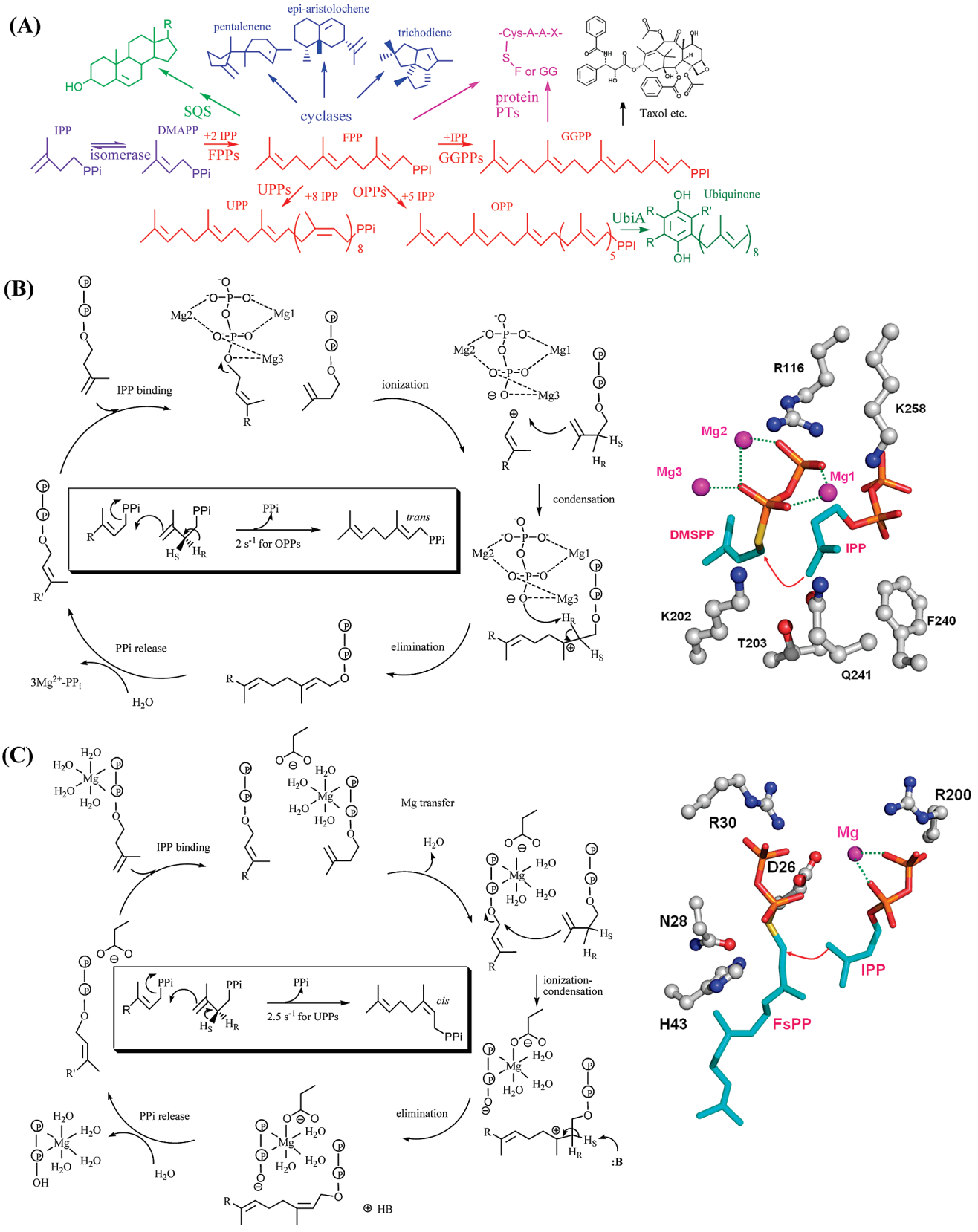

FIGURE 1: Biosynthesis of isoprenoids and proposed mechanisms for *trans*- and *cis*-prenyltransferases. (A) FPP is synthesized from DMAPP and IPP and serves as a branching point leading to a variety of isoprenoids. The prenyltransferases are grouped in different colors. (B) The reactions of *trans*-prenyltransferases proceed with the ionization, condensation, and elimination sequential mechanism. Diphosphate is dissociated from FPP to form a carbocation, which is then condensed with IPP, and the H_R proton is eliminated from IPP to form the condensation adduct. The rate constant of IPP condensation for OPPs is 2 s^{-1} (center). The active-site structure of FPPs (PDB entry 1RQI) is shown in the right panel. (C) In *cis*-prenyltransferase reactions, dissociation of diphosphate occurs with IPP condensation in a concerted way, and then the H_S is eliminated from IPP by a general base to form the condensation adduct. The rate constant of IPP condensation for UPPs is 2.5 s^{-1} (center). The active-site structure of UPPs (PDB entry 1X06) is shown in the right panel.

which FPP can first bind to UPPs without Mg^{2+} and the MgIPP complex from the solution is then bound to the enzyme, allowing the Mg^{2+} to shift its position toward FPP diphosphate and facilitate the concerted FPP diphosphate dissociation and IPP attack (see the left panel of Figure 1C for the mechanism). Next, Asn74 or Ser71 in *E. coli* UPPs may act as a general base to remove the H_S from the C2 atom of IPP according to the crystal structures. The carboxyl group of Asp26 assists the migration of Mg^{2+} from IPP to FPP. Unlike in the *trans*-prenyltransferases where multiple Mg^{2+} ions are fixed with several Asp residues from the two conserved DDxxD motifs, the Mg^{2+} chelated by only one Asp residue is more mobile in catalyzing the UPPs reaction.

Similar to the *trans*-prenyltransferases, the evidence of carbocation formation for the allylic substrates was observed in the prenyltransferases which catalyze FPP cyclization such as pentalenene synthase (*41*), epi-aristolochene synthase (*42*), aristolochene synthase (*43*), and trichodiene synthase (*44*) as well as those catalyze two-FPP condensation such as squalene synthase (*45*) and protein prenyltransferases which catalyze the transfer of the farnesyl or geranylgeranyl group to cellular proteins at a Cys residue near their carboxyl termini (*46*). The diphosphate group of their FPP substrate is bound either through a metal ion (Mg^{2+} required) coordinated by the Asp-rich motifs or via the positively charged and H-bond-forming amino acids (Mg^{2+} not required) in the active sites, as both modes existing in the *trans*-prenyltransferases for FPP and IPP binding, respectively.

CHAIN-LENGTH DETERMINATION MECHANISMS

cis- and *trans*-prenyltransferases generate products with correct chain lengths according to a molecular ruler mechanism, where one or two bulky amino acids occupy the bottom of each of the enzyme active sites to block extra chain elongation of the products, thereby determining the ultimate chain lengths. As revealed by their three-dimensional structures (*28*−*35*), the distances between the first Asp of the first DDxxD motif where the allylic substrate is bound and F113, W74, V178/D182, Y107/H139, L164, and F132 at the lower positions of the active-site crevices in avian FPPs, *Thermus thermophilus* type I GGPPs, *Salix alba* (mustard) type II, *S. cerevisiae* type-III GGPPs, *Solfolobus solfataricus* HexPPs, and *Thermotoga maritima* OPPs, respectively, are increasing with longer product chain lengths. GGPPs are classified into three types based on their amino acid sequences: type I GGPPs contains a large amino acid at the fourth or fifth position prior to the DDxxD motif, but type II (with insertion of two amino acids within the first Asp-rich motif) and type III GGPPs found in eukaryotes (except plants) have a small amino acid at the corresponding position (*47*). These bulky amino acids at the bottom of active sites are proposed as "floors" and can be provided from different secondary structural elements. As illustrated in Figure 2A, the floor is located at helix D for FPPs and type-I GGPPs, but in helix F and G for type-II and type-III GGPPs, and in helix G for OPPs and HexPPs. Site-directed mutagenesis studies have proven that substitution of these floors with small amino acids yields longer products (*29*, *30*, *33*, *48*). A "molecular ruler" hypothesis was proposed for protein prenyltransferases to distinguish between FPP and GGPP substrates, suggesting it is a general concept for enzymes that synthesize or transfer hydrocarbons of various chain lengths (*49*).

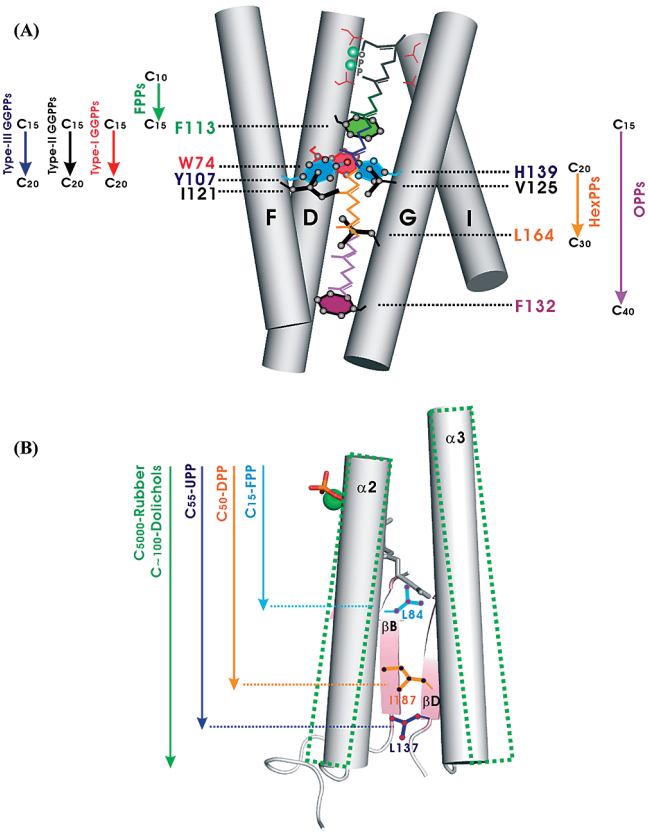

FIGURE 2: Molecular ruler mechanism of chain-length determination for *trans*- and *cis*-prenyltransferases. (A) Common active-site crevice surrounded by helices D, F, and G with the bulky amino acids at the bottom for different *trans*-prenyltransferases. The key residues for chain-length determination are F113 for C_{15} avian FPPs (PDB entry 1FPS), W74 for C_{20} *T. thermophilus* type I GGPPs (PDB entry 1WMW), I121/V125 for C_{20} *Pantoea ananatis* type II GGPPs (PDB entry 2J1P), Y107/H139 for C_{20} *S. cerevisiae* type III GGPPs (PDB entry 2DH4), L164 for C_{30} *Sol. solfataricus* HexPPs (PDB entry 2AZJ), and F132 for C_{40} *T. maritima* OPPs (PDB entry 1V4E), which are colored green, red, black, cyan, orange, and purple, respectively. (B) Bulky amino acids for determining the chain length of *cis*-prenyltransferases. L137 (blue) serves as a key residue for determining the chain length of *E. coli* UPPs and I187 (orange) for *cis*-DPPs, whereas the floor is Leu84 (cyan) for the short-chain *cis*-FPPs. Rubber prenyltransferase contains a three-amino acid insertion in α3, causing expansion of the opening (shown as green dashed lines).

In *E. coli* UPPs, replacement of a large L137 at the bottom of an active site with a small Ala results in a larger product, indicating L137 as the floor (*37*) (Figure 2B). I187 in *M. tuberculosis* decaprenyl diphosphate synthase (DPPs), which corresponds to L137 in *E. coli* UPPs, controls the C_{50} chain length (our unpublished results). The unusual short-chain FPP catalyzed by the *M. tuberculosis cis*-FPPs may be shielded by Leu84 in *β*B near the top of the tunnel based on the crystal structure (*50*) (Figure 2B). The site-directed mutagenesis study shows that the L84A mutant *cis*-FPPs produced a product longer than that of the wild type, confirming Leu84 plays an important role in product chain-length determination (*51*). Replacement of the corresponding A69 in *E. coli* UPPs or A72 in *Micrococcus luteus* B-P 26 UPPs with Leu also results in shorter-chain-length products (*37*, *52*). For rubber prenyltransferase to yield a polymer with almost unlimited chain length, it was suggested that three amino acid residues inserted into the α3 helix sequence extend the bottom loop which results in the required increase in tunnel volume (*53*). Yeast Srt1p and Rer2p and human dehydrodolichyl

diphosphate synthases, which synthesize products longer than UPPs, also have three- to five-amino acid insertions in this region. The recombinant UPPs mutants with insertion of these amino acids gave longer products (*52*).

CONFORMATIONAL CHANGES

In *trans*-prenyltransferases, compared to the unliganded structure of *Staphylococcus aureus* FPPs, the structure of the *E. coli* FPPs−IPP−DMSPP ternary complex reveals significant substrate-induced active-site rearrangements (*31*). Notably, conserved Arg116 and Lys258 emanating from the conformationally variable αD−αE and αH−αI loops in FPPs shield the reaction from bulk solvent and stabilize the catalytic base of pyrophosphate oxygen by their positive charges. A similar conformation in the αD−αE loop can be found in monomer A of HexPPs (*32*). On the basis of the two conformers observed in HexPPs and the FPPs−substrate complex, monomer A with the inward αD−αE loop represents a substrate-free conformation (Figure 3A). As the substrates bind, the αH−αJ loop moves inward toward the active site to facilitate catalysis involving with the positively charged amino acids (R90 and R91). When the product is formed, the αD−αE and αH−αJ loops at the top of the active site move away from the closed position to the open position and the flexible regions (αI, αJ, and αK) move outward for product release (Figure 3A).

For *E. coli* UPPs, three major conformers were observed as shown in Figure 3B, where the apoenzyme has a disordered loop (*37*), the FPP-bound enzyme adopts a closed form with helix α3 more kinked toward the bound substrate (*39*, *40*), and the product-bound enzyme (with two Triton molecules to mimic the product) displays an open form (*38*). The loop (amino acids 72−82) connecting helix α3 and *β*B is highly flexible, so its electron density is invisible in the apo-UPPs structure but becomes ordered once FPP is bound. The conformational change is critical for catalysis as the open conformation fixed by the insertion or deletion of amino acids in this loop region impedes the enzyme activity by 10^4-fold (*54*). Fluorescence stopped-flow technology has been utilized to observe the conformational changes from the apo form to the closed form by substrate binding and then to the open form by the crowding of the long-chain product, as shown by a three-phase trace (*55*).

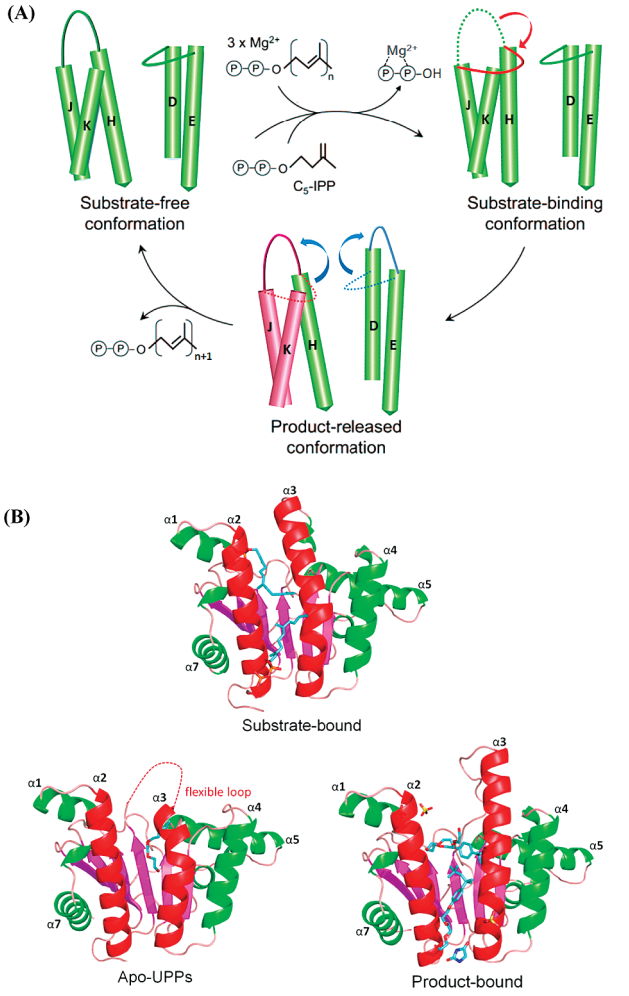

FIGURE 3: Conformational changes of (A) *trans*-type HexPPs and (B) *cis*-type UPPs. (A) In HexPPs and FPPs, substrate binding and product release might trigger the movement of the αD−αE and αH−αJ loops toward and away from the active site, respectively. Helices J and K (colored pink) are highly flexible. In panel B, upon FPP binding, UPPs undergoes a conformational change in helix α3 that is more kinked in the substrate-bound form (closed form), but a portion of electron density in a flexible loop is invisible in the apoenzyme. In the product-bound form, an open conformation is formed, where helix α3 is relatively straight. The structures of apo-UPPs, FPP-bound UPPs, and Triton-bound UPPs were taken from PDB entries 1JP3, 1V7U, and 1UEH, respectively.

INHIBITOR DESIGN

FPPs was recently identified as a target for the bisphosphonate drugs risedronate and zoledronate used to treat bone resorption diseases such as osteoporesis due to its functions in cell signaling pathways by producing FPP for prenylation of small GTPases (*56*, *57*). However, GGPPs was also proposed as the main target for the most potent bisphosphonate zoledronate (Zometa) in human cells (*58*). While bisphosphonates inhibit the *trans*-prenyltransferases by mimicking the diphosphate headgroup of allylic substrates, it was found that some of these compounds with more bulky side chains can potently inhibit *cis*-type UPPs (*59*). However, different binding modes were found as revealed by the crystal structures of human FPPs, *Trypanosoma cruzi* FPPs, *S. cerevisiae* GGPPs, and *E. coli* UPPs in complex with the bisphosphonate inhibitors (*59*−*61*).

Unlike the single bisphosphonate binding mode in FPPs (diphosphate moieties bind in the DMAPP site), the complexed structures of yeast GGPPs with the bisphosphonates (chemical structures shown in Figure 4A) and product display four different binding modes (diphosphate moieties can bind in either the FPP or IPP sites) as shown in Figure 4B (*59*). The small bisphosphonates including zoledronate and minodronate and the larger BPH-629 bind in a manner similar to that of FPP (F***PP-F***PP mode). Large bisphosphonate inhibitors with long hydrophobic side chains such as BPH-675 bind like human GGPP product in the F***PP-GG***PP mode, where the charged headgroup occupies the diphosphate-binding site of FPP and the hydrophobic side chains in the "inhibition site" identified in human GGPPs (*53*). BPH-629 also binds to yeast GGPP in another mode called I***PP-GG***PP since its headgroup occupies the diphosphate-binding site of IPP and its side chain extends to the inhibitor site. Two molecules of the inhibitor are bound in two different modes, indicating higher flexibility of the GGPPs active site compared to that of FPPs. The product in yeast GGPPs is bound in an I***PP-F***PP mode, with its diphosphate group in the IPP site and the C_{20} side chain in the FPP site. Furthermore, diprenyl methylenebisphosphonates, such as digeranyl methylene

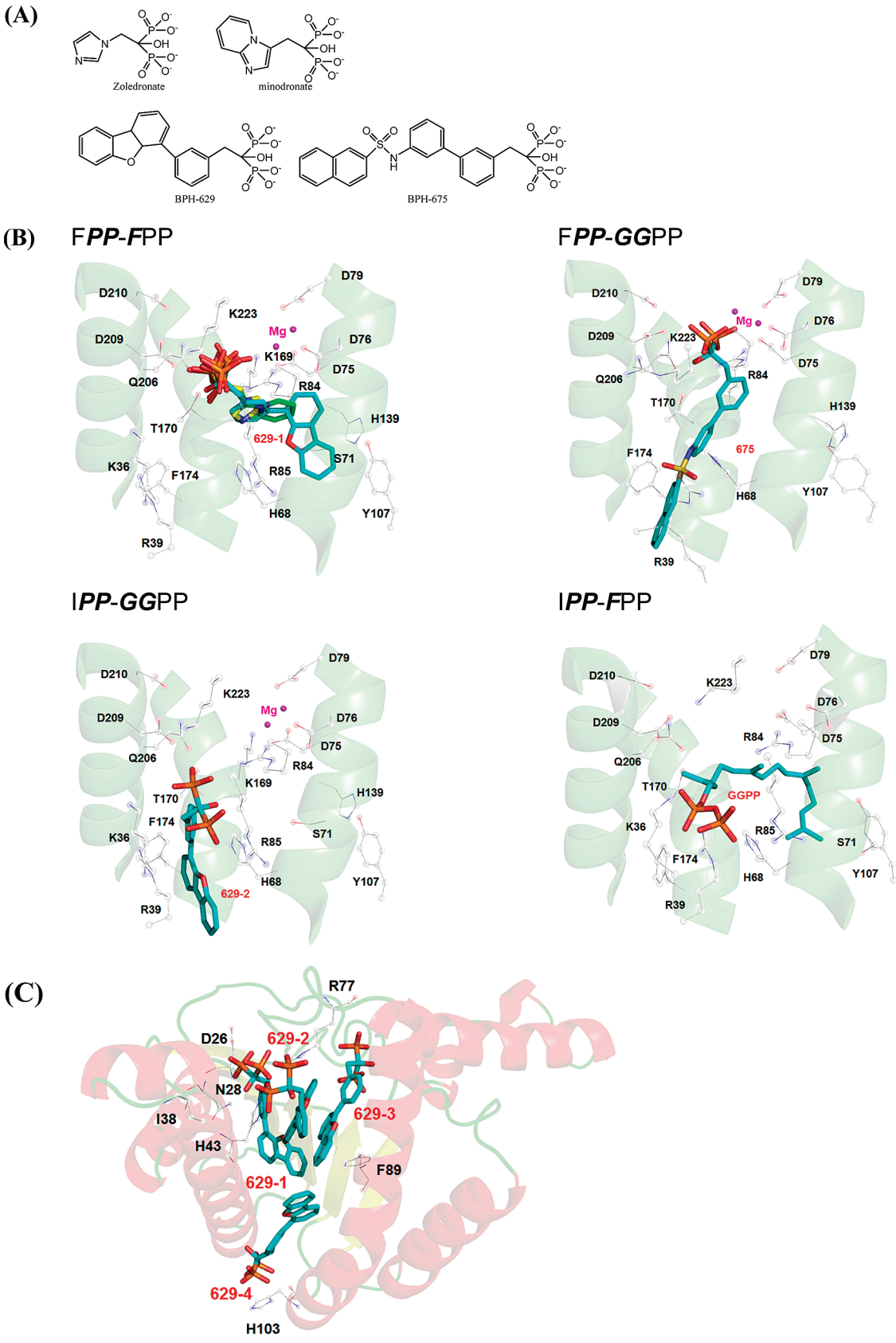

FIGURE 4: Bisphosphonate inhibitors and their binding modes with *trans*-GGPPs and *cis*-UPPs. (A) Two small bisphosphonate drugs, zoledronate and minodronate, and two bulky bisphosphonates with hydrophobic side chains are shown. (B) Complexed yeast GGPPs structures showing four binding modes: F***PP-FPP*** (with zoledronate colored yellow, PDB entry 2E91; with minodronate colored green, PDB entry 2E92; with 629-1, PDB entry 2E93), F***PP-GG***PP (with 675, PDB entry 2E95), I***PP***-GGPP (with 629-2, PDB entry 2E93), and I***PP-FPP*** (with product, PDB entry 2E8V). (C) In the UPPs active site, four molecules of BPH-629 are bound (PDB entry 2E98).

bisphosphonate, have potent activity against GGPPs, and thus against the K562 tumor cell line (*62*). Crystallographic studies show these V-shaped bisphosphonates bind to both the FPP and GGPP sites (*63*).

The bisphosphonate compounds with hydrophobic side chains also bind to UPPs. Because of the large space of the UPPs active site, there are four binding sites per monomer of the UPPs for an inhibitor BPH-629, three of which occupy the top of the active site, and the fourth site is situated at the bottom (Figure 4C) (*59*). Four molecules of the inhibitor were found in chain A, whereas only one complete molecule and two partial molecules were observed in chain B. When all bisphosphonate complex structures are superimposed on the UPPs−Mg−FsPP−IPP structure, the width (10.3−12.9 Å) and length (21−25.2 Å) of the funnel-shaped hydrophobic tunnel are well-defined. Among the four sites, site 1 corresponds to the FPP (FsPP) substrate binding site.

Bisphosphonates are potential inhibitors for other prenyltransferases. Recently, it was found that a bisphosphonate which acts as a cholesterol biosynthesis inhibitor, an inhibitor of human squalene synthase (SQS), can also block *St. aureus* virulence by inhibiting its dehydrosqualene synthase (CrtM) (*64*). Both CrtM and SQS catalyze the condensation of two FPP, leading to dehydrosqualene as the precursor of staphyloxanthin in *St. aureus* and squalene as a precursor of cholesterol in humans, respectively, and they also share similar structures.

Some potent inhibitors other than bisphosphonate-related compounds are under development. It was reported recently that tetramic, tetronic, and dihydropyridin-2-ones are potent and selected inhibitors of UPPs (*65*). Computer screening also identified inhibitors which exhibit differential activities against *Helicobacter pylori* and *E. coli* UPPs, although their potency has to be improved (*66*).

CONCLUSION AND FUTURE DIRECTIONS

This review summarizes the kinetics, mechanisms, structures, and inhibitors of the *cis*- and *trans*-prenyltransferases which synthesize linear products by condensation with IPP toward specific chain lengths. Like *trans*-prenyltransferases, FPP cyclases and squalene synthases require Mg^{2+} for activity and contain Asp-rich binding motifs, which support their common evolutionary origin. However, *cis*-prenyltransferases utilize a Mg^{2+} chelated by a P-loop that is shared by many phosphate-binding proteins for phosphate binding (*67*), suggesting they are evolutionarily distinct from the prenyltransferases containing Asp-rich motifs. Protein prenyltransferases do not contain Asp-rich motifs and do not require Mg^{2+} for binding with the FPP or GGPP substrate, although a high concentration of Mg^{2+} can increase the enzyme activity by 700-fold (*68*). Recently, a few aromatic prenyltransferases which catalyze the transfer of allylic isoprenyl moieties (DMAPP or GPP) to aromatic acceptors were identified in the biosynthetic pathways of secondary metabolites in plants, fungi, and bacteria (*69*, *70*). Unlike the membrane-bound aromatic prenyltransferases of ubiquinone biosynthesis such as UbiA in *E. coli*, which transfers oligoprenyl groups to 4-hydroxybenzoate using an Asp-rich motif (e.g., NDxxDxxxD) and Mg^{2+} (*71*), CloQ, which is involved in the biosynthesis of clorobiocin via catalysis of a C-prenylation at position 3 of 4-hydroxyphenylpyruvate using DMAPP as the prenyl donor, does not contain an Asp-rich motif and does not require a metal ion for activity (*72*). However, naphthalene prenyltransferase (NphB), which catalyzes C-geranylation of the artificial substrate 1,6-dihydroxynaphthalene and of other phenolic substrates, has sequence similarity with CloQ (also without the DDxxD motif) but requires Mg^{2+} for activity, which is coordinated by four water molecules, one of the GPP α-phosphate oxygens, and one Asp based on the crystal structure (*73*).

Substrate-induced conformational changes are often associated with the prenyltransferases. The most well characterized conformational change is for *cis*-prenyltransferase UPPs, and this conformational change is essential for catalysis. The *trans*-type FPPs also undergoes a conformational change upon substrate binding, as does HexPPs. However, biochemical evidence is needed to show the importance of the conformational change in catalysis.

There has been considerable interest in developing specific inhibitors of some of the prenyltransferases for diseases. However, so far, only bisphosphonates are potent and useful inhibitors targeting FPPs and GGPPs. More effort needs to be spent in developing new classes of selective and potent inhibitors against disease-related prenyltransferases.

In summary, we have updated our knowledge of the prenyltransferases which make linear products using allylic diphosphates and IPP substrates. There are many other prenyltransferases which are responsible for making a variety of important isoprenoids still not well characterized and deserve further study.

ACKNOWLEDGMENT

I deeply thank former co-workers who contributed to the work from our laboratories.

REFERENCES

1. Poulter, C. D., and Rilling, H. C. (1981) in Biosynthesis of isoprenoid compounds (Spurgeon, S. R., Ed.) Vol. 1, pp 1−282, John Wiley & Sons, New York.
2. Ogura, K., Koyama, T., and Sagami, H. (1997) in Subcellular Biochemistry (Bittman, R., Ed.) Vol. 28, pp 57−88, Plenum, New York.
3. Thulasiram, H. V., Erickson, H. K., and Poulter, C. D. (2007) Chimeras of two isoprenoid synthases catalyze all four coupling reactions in isoprenoid biosynthesis. *Science 316*, 73–76.
4. Rohmer, M., Knani, M., Simonin, P., Sutter, B., and Sahm, H. (1993) Isoprenoid biosynthesis in bacteria: A novel pathway for the early steps leading to isopentenyl diphosphate. *Biochem. J. 295*, 517–524.
5. Arigoni, D., Sagner, S., Latzel, C., Eisenreich, W., Bacher, A., and Zenk, M. H. (1997) Terpenoid biosynthesis from 1-deoxy-D-xylulose in higher plants by intramolecular skeletal rearrangement. *Proc. Natl. Acad. Sci. U.S.A. 94*, 10600–10605.
6. Durbecq, V., Sainz, G., Oudjama, Y., Clantin, B., Bompard-Gilles, C., Tricot, C., Caillet, J., Stalon, V., Droogmans, L., and Villeret, V. (2001) Crystal structure of isopentenyl diphosphate:dimethylallyl diphosphate isomerase. *EMBO J. 20*, 1530–1537.
7. Sacchettini, J. C., and Poulter, C. D. (1997) Creating isoprenoid diversity. *Science 277*, 1788–1789.
8. Kellogg, B. A., and Poulter, C. D. (1997) Chain elongation in the isoprenoid biosynthetic pathway. *Curr. Opin. Chem. Biol. 1*, 570–578.
9. Ogura, K., and Koyama, T. (1998) Enzymatic aspects of isoprenoid chain elongation. *Chem. Rev. 98*, 1263–1276.
10. Liang, P. H., Ko, T. P., and Wang, A. H. (2002) Structures, mechanisms, and functions of prenyltransferases. *Eur. J. Biochem. 269*, 3339–3354.
11. Clarke, S. (1992) Protein isoprenylation and methylation at carboxy-terminal cysteine residue. *Annu. Rev. Biochem. 61*, 355–386.
12. Sanders, J. M., Song, Y., Chan, J. M., Zhang, Y., Jennings, S., Kosztowski, T., Odeh, S., Flessner, R., Schwerdtfeger, C., Kotsikorou, E., Meints, G. A., Gomez, A. O., Gonzalez,-Pacanowska, D., Raker, A. M., Wang, H., van Beek, E. R., Papapoulos, S. E., Morita, C. T., and Oldfield, E. (2005) Pyridinium-1-yl Bisphosphonates Are Potent Inhibitors of Farnesyl Diphosphate Synthase and Bone Resorption. *J. Med. Chem. 48*, 2957–2963.
13. Wang, K., and Ohnuma, S. (1999) Chain-length determination mechanism of isoprenyl diphosphate synthases and implications for molecular evolution. *Trends Biochem. Sci. 24*, 445–451.
14. Schulbach, M. C., Brennan, P. J., and Crick, D. C. (2000) Identification of a short (C_{15}) chain Z-isoprenyl diphosphate synthase and a

homologous long (C_{50}) chain isoprenyl diphosphate synthase in *Mycobacterium tuberculosis*. *J. Biol. Chem. 275*, 22876–22881.
15. Allen, C. M. (1985) Purification and characterization of undecaprenyl pyrophosphate synthase. *Methods Enzymol. 110*, 281–299.
16. Bouhss, A., Trunkfield, A. E., Bugg, T. D., and Mengin-Lecreulx, D. (2008) The biosynthesis of peptidoglycan lipid-linked intermediates. *FEMS Microbiol. Rev. 32*, 208–233.
17. Sato, M., Sato, K., Nishikawa, S., Hirata, A., Kato, J., and Nakano, A. (1999) The yeast RER2 gene, identified by endoplasmic reticulum protein localization mutations, encodes cis-prenyltransferase, a key enzyme in dolichol synthesis. *Mol. Cell. Biol. 19*, 471–483.
18. Cornish, K. (1993) The separate roles of plant cis and trans prenyl transferases in cis-1,4-polyisoprene biosynthesis. *Eur. J. Biochem. 218*, 267–271.
19. Pan, J. J., Chiu, S. T., and Liang, P. H. (2000) Product distribution and pre-steady-state kinetic analysis of *Escherichia coli* undecaprenyl pyrophosphate synthase reaction. *Biochemistry 39*, 10936–10942.
20. Pan, J. J., Kuo, T. H., Chen, Y. K., Yang, L. W., and Liang, P. H. (2002) Insight into the activation mechanism of *Escherichia coli* octaprenyl derived from pre-steady-state kinetic analysis. *Biochim. Biophys. Acta 1594*, 64–73.
21. Chen, A. P., Chen, Y. H., Liu, H. P., Li, Y. C., Chen, C. T., and Liang, P. H. (2002) Synthesis and application of a fluorescent substrate analogue to study ligand interactions for undecaprenyl pyrophosphate synthase. *J. Am. Chem. Soc. 124*, 15217–15224.
22. Pan, J. J., Yang, L. W., and Liang, P. H. (2000) Effect of site-directed mutagenesis of the conserved aspartate and glutamate on *E. coli* undecaprenyl pyrophosphate synthase catalysis. *Biochemistry 39*, 13856–13861.
23. Poulter, C. D., and Rilling, H. C. (1978) The prenyl transfer reaction. Enzymic and mechanistic studies of the 1′-4 coupling reaction in the terpene biosynthetic pathway. *Acc. Chem. Res. 11*, 307–313.
24. Poulter, C. D., Argyle, J. C., and Mash, E. A. (1977) Letter: Prenyltransferase. New evidence for an ionization-condensation-elimination mechanism with 2-fluorogeranyl pyrophosphate. *J. Am. Chem. Soc. 99*, 957–959.
25. Lu, Y. P., Liu, H. G., and Liang, P. H. (2009) Different reaction mechanisms for cis- and trans-prenyltransferases. *Biochem. Biophys. Res. Commun. 379*, 351–355.
26. Shimizu, N., Koyama, T., and Ogura, K. (1998) Molecular cloning, expression, and purification of undecaprenyl diphosphate synthase. No sequence similarity between E- and Z-prenyl diphosphate synthases. *J. Biol. Chem. 273*, 19476–19481.
27. Apfel, C. M., Takacs, B., Fountoulakis, M., Stieger, M., and Keck, W. (1999) Use of genomics to identify bacterial undecaprenyl pyrophosphate synthetase: Cloning, expression, and characterization of the essential uppS gene. *J. Bacteriol. 181*, 483–492.
28. Tarshis, L. C., Yan, M., Poulter, C. D., and Sacchettini, J. C. (1994) Crystal structure of recombinant farnesyl diphosphate synthase at 2.6-Å resolution. *Biochemistry 33*, 10871–10877.
29. Tarshis, L. C., Proteau, P. J., Kellogg, B. A., Sacchettini, J. C., and Pouter, C. D. (1996) Regulation of product chain length by isoprenyl diphosphate synthases. *Proc. Natl. Acad. Sci. U.S.A. 93*, 15018–15023.
30. Guo, R. T., Kuo, C. J., Chou, C. C., Ko, T. P., Shr, H. L., Liang, P. H., and Wang, A. H. (2004) Crystal structure of octaprenyl pyrophosphate synthase from hyperthermophilic *Thermotoga maritima* and mechanism of product chain length determination. *J. Biol. Chem. 279*, 4903–4912.
31. Hosfield, D. J., Zhang, Y., Dougan, D. R., Broun, A., Tari, L. W., Swanson, R. V., and Finn, J. (2004) Structural basis for bisphosphonate-mediated inhibition of isoprenoid biosynthesis. *J. Biol. Chem. 279*, 8526–8529.
32. Sun, H. Y., Ko, T. P., Kuo, C. J., Guo, R. T., Chou, C. C., Liang, P. H., and Wang, A. H. (2005) Homo-dimeric hexaprenyl pyrophosphate synthase from Thermoacidophilic Crenarchaeon *Sulfolobus solfataricus* displays asymmetric subunit structures. *J. Bacteriol. 187*, 8137–8148.
33. Chang, T. H., Guo, R. T., Ko, T. P., Wang, A. H., and Liang, P. H. (2006) Crystal structure of type-III geranylgeranyl pyrophosphate synthase from *Saccharomyces cerevisiae* and the mechanism of product chain length determination. *J. Biol. Chem. 281*, 14991–15000.
34. Kavanagh, K. L., Dunford, J. E., Bunkoczi, G., Russell, R. G., and Oppermann, U. (2006) The crystal structure of human geranylgeranyl pyrophosphate synthase reveals a novel hexameric arrangement and inhibitory product binding. *J. Biol. Chem. 281*, 22004–22012.
35. Kloer, D. P., Welsch, R., Beyer, P., and Schulz, G. E. (2006) Structure and reaction geometry of geranylgeranyl diphosphate synthase from *Sinapis alba*. *Biochemistry 45*, 15197–15204.
36. Fujihashi, M., Zhang, Y.-W., Higuchi, Y., Li, X.-Y., Koyama, T., and Miki, K. (2001) Crystal structure of cis-prenyl chain elongating enzyme, undecaprenyl diphosphate synthase. *Proc. Natl. Acad. Sci. U.S.A. 98*, 4337–4342.
37. Ko, T. P., Chen, Y. K., Robinson, H., Tsai, P. C., Gao, Y. G., Chen, A. P., Wang, A. H., and Liang, P. H. (2001) Mechanism of product chain length determination and the role of a flexible loop in *E. coli* undecaprenyl pyrophosphate synthase catalysis. *J. Biol. Chem. 276*, 47474–47482.
38. Chang, S. Y., Ko, T. P., Liang, P. H., and Wang, A. H. (2003) Catalytic mechanism revealed by the crystal structure of undecaprenyl pyrophosphate synthase in complex with sulfate, magnesium, and triton. *J. Biol. Chem. 278*, 29298–29307.
39. Chang, S. Y., Ko, T. P., Chen, A. P., Wang, A. H., and Liang, P. H. (2004) Substrate binding mode and reaction mechanism of undecaprenyl pyrophosphate synthase deduced from crystallographic studies. *Protein Sci. 13*, 971–978.
40. Guo, R. T., Ko, T. P., Chen, A. P., Kuo, C. J., Wang, A. H., and Liang, P. H. (2005) Crystal structures of undecaprenyl pyrophosphate synthase in complex with magnesium, isopentenyl pyrophosphate and farnesyl thiopyrophosphate: Roles of the metal ion and conserved residues in catalysis. *J. Biol. Chem. 280*, 20762–20774.
41. Lesburg, C. A., Zhai, G., Cane, D. E., and Christianson, D. W. (1997) Crystal structure of pentalenene synthase: Mechanistic insights on terpenoid cyclization reactions in biology. *Science 275*, 1820–1824.
42. Starks, C. M., Back, K., Chappell, J., and Noel, J. P. (1997) Structural basis for cyclic terpene biosynthesis by tobacco 5-epi-aristolochene synthase. *Science 275*, 1815–1820.
43. Caruthers, J. M., Kang, I., Rynkiewicz, M. J., Cane, D. E., and Christianson, D. W. (2000) Crystal structure determination of aristolochene synthase from the blue cheese mold, *Penicillium roqueforti*. *J. Biol. Chem. 275*, 25533–25539.
44. Rynkiewicz, M. J., Cane, D. E., and Christianson, D. W. (2001) Structure of trichodiene synthase from *Fusarium sporotrichioides* provides mechanistic inferences on the terpene cyclization cascade. *Proc. Natl. Acad. Sci. U.S.A. 98*, 13543–13548.
45. Pandit, J., Danley, D. E., Schulte, G. K., Mazzalupo, S., Pauly, T. A., Hayward, C. M., Hamanaka, E. S., Thompson, J. F., and Horwood, H. J. (2000) Crystal structure of human squalene synthase. A key enzyme in cholesterol biosynthesis. *J. Biol. Chem. 275*, 30610–30617.
46. Park, H.-W., Boduluri, S. R., Moomaw, J. F., Casey, P. J., and Beese, L. S. (1997) Crystal structure of protein farnesyltransferase at 2.25 angstrom resolution. *Science 275*, 1800–1804.
47. Hemmi, H., Noike, M., Nakayama, T., and Nishino, T. (2003) An alternative mechanism of product chain-length determination in type III geranylgeranyl diphosphate synthase. *Eur. J. Biochem. 270*, 2186–2194.
48. Noike, M., Katagiri, T., Nakayama, T., Koyama, T., Nishino, T., and Hemmi, H. (2008) The product chain length determination mechanism of type II geranylgeranyl diphosphate synthase requires subunit interaction. *FEBS J. 275*, 3921–3933.
49. Long, S. B., Casey, P. J., and Beese, L. S. (1998) Cocrystal structure of protein farnesyltransferase complexed with a farnesyl diphosphate substrate. *Biochemistry 37*, 9612–9618.
50. Wang, W., Dong, C., McNeil, M., Kaur, D., Mahapatra, S., Crick, D. C., and Naismith, J. H. (2008) The structural basis of chain length control in Rv1086. *J. Mol. Biol. 381*, 129–140.
51. Noike, M., Ambo, T., Kikuchi, S., Suzuki, T., Yamashita, S., Takahashi, S., Kurokawa, H., Mahapatra, S., Crick, D. C., and Koyama, T. (2008) Product chain-length determination mechanism of Z,E-farnesyl diphosphate synthase. *Biochem. Biophys. Res. Commun. 377*, 17–22.
52. Kharel, Y., Takahashi, S., Yamashita, S., and Koyama, T. (2006) Manipulation of prenyl chain elongation determination mechanism of cis-prenyltransferases. *FEBS J. 273*, 647–657.
53. Poznański, J., and Szkopinska, A. (2007) Precise bacterial polyprenol length control fails in *Saccharomyces cerevisiae*. *Biopolymers 86*, 155–164.
54. Chang, S. Y., Chen, Y. K., Wang, A. H.-J., and Liang, P. H. (2003) Identification of the active conformation and the importance of length of the flexible loop 72−83 in regulating the conformational change of undecaprenyl pyrophosphate synthase. *Biochemistry 42*, 14452–14459.
55. Chen, Y. H., Chen, A. P., Chen, C. T., Wang, A. H., and Liang, P. H. (2002) Probing the conformational change of *Escherichia coli* undecaprenyl pyrophosphate synthase during catalysis using an inhibitor and tryptophan mutants. *J. Biol. Chem. 277*, 7369–7376.
56. Bergstrom, J. D., Bostedor, R. G., Masarachia, P. J., Reszka, A. A., and Rodan, G. (2000) Alendronate is a specific nanomolar inhibitor

of farnesyl diphosphate synthase. *Arch. Biochem. Biophys. 373*, 231–241.
57. Dunford, J. E., Thompson, K., Coxon, F. P., Luckman, S. P., Hahn, F. M., Poulter, C. D., Ebetino, F. H., and Rogers, M. J. (2001) Structure-activity relationships for inhibition of farnesyl diphosphate synthase in vitro and inhibition of bone resorption in vivo by nitrogen-containing bisphosphonates. *J. Pharm. Exp. Ther. 296*, 235–242.
58. Goffinet, M., Thoulouzan, M., Pradines, A., Lajoie-Mazenc, I., Weibaum, C., Faye, J. C., and Seronie-Vivien, S. (2006) Zoledronic acid treatment impairs protein geranylgeranylation for biological effects in prostatic cell. *BMC Cancer 6*, 60.
59. Guo, R. T., Cao, R., Liang, P. H., Ko, T. P., Chang, T. H., Hudock, M., Jeng, W. Y., Chen, C. K., Zhang, Y., Song, Y., Kuo, C. J., Yin, F., Oldfield, E., and Wang, A. H. (2007) Bisphosphonates target multiple sites in both *cis*- and *trans*-prenyltransferases: A crystallographic investigation. *Proc. Natl. Acad. Sci. U.S.A. 104*, 10022–10027.
60. Kavanagh, K. L., Guo, K., Dunfold, J. E., Wu, X., Knapp, S., Ebetino, F. H., Rogers, M. J., Russell, R. G., and Oppermann, U. (2006) The molecular mechanism of nitrogen-containing bisphosphonates as antiosteoporosis drugs. *Proc. Natl. Acad. Sci. U.S.A. 103*, 7829–7834.
61. Gabelli, S. B., McLellan, J. S., Montalvetti, A., Oldfield, E., Docampo, R., and Amzel, L. M. (2006) Structure and mechanism of farnesyl diphosphate synthase from *Tryposoma cruzi*: Implications for drug design. *Proteins 62*, 80–88.
62. Wiemer, A. J., Tong, H., Swanson, K. M., and Hohl, R. J. (2007) Digeranyl bisphosphonates inhibits geranylgeranyl pyrophosphate synthase. *Biochem. Biophys. Res. Commun. 353*, 921–925.
63. Chen, C. K., Hudock, M. P., Zhang, Y., Kuo, R. T., Cao, R., No, J. H., Liang, P. H., Ko, T. P., Chang, T. H., Chang, S. C., Song, Y., Axelson, J., Kumar, A., Wang, A. H., and Oldfield, A. (2008) Inhibition of geranylgeranyl diphosphate synthase by bisphosphonates: A crystallographic and computational investigation. *J. Med. Chem. 51*, 5594–5607.
64. Liu, C. I., Liu, G. Y., Song, Y., Yin, F., Hensler, M. E., Jeng, W. Y., Nizet, V., Wang, A. H., and Oldfield, E. (2008) A cholesterol biosynthesis inhibitor blocks *Staphylococcus aureus* virulence. *Science 319*, 1391–1394.
65. Peukert, S., Sun, Y., Zhang, R., Hurley, B., Sabio, M., Shen, X., Gray, C., Dzink-Fox, J., Tao, J., Cebula, R., and Wattanasin, S. (2008) Design and structure-activity relationships of potent and selective inhibitors of undecaprenyl pyrophosphate synthase (UPPS): Tetramic, tetronic acids and dihydropyridin-2-ones. *Bioorg. Med. Chem. Lett. 18*, 1840–1844.
66. Kuo, C. J., Guo, R. T., Lu, I. L., Liu, H. G., Wu, S. Y., Ko, T. P., Wang, A. H., and Liang, P. H. (2008) Structure-based inhibitors exhibit differential activities against *Helicobacter pylori* and *Escherichia coli* undecaprenyl pyrophosphate synthases. *J. Biomed. Biotechnol. 2008*, 841312.
67. Kinoshita, K., Sadanami, K., Kidera, A., and Go, N. (1999) Structural motif of phosphate-binding site common to various protein superfamilies: All-against-all structural comparison of protein-mononucleotide complexes. *Protein Eng. 12*, 11–14.
68. Saderholm, M. J., Hightower, K. E., and Fierke, C. A. (2000) Role of metals in the reaction catalyzed by protein farnesyltransferase. *Biochemistry 39*, 12398–12405.
69. Heide, L. (2009) Prenyl transfer to aromatic substrates: Genetics and enzymology. *Curr. Opin. Chem. Biol. 13*, 171–179.
70. Li, S. M. (2009) Evolution of aromatic prenyltransferases in the biosynthesis of indole derivatives. *Phytochemistry* (in press).
71. Melzer, M., and Heide, L. (1994) Charazterization of polyprenyldiphosphate:4-hydroxybenzoate polyprenyltransferase from *Escherichia coli*. *Biochim. Biophys. Acta 1212*, 93–102.
72. Pojer, F., Wemakor, E., Kammerer, B., Chen, H., Walsh, C. T., Li, S. M., and Heide, L. (2003) CloQ, a prenyltransferase involved in chlorobiocin biosynthesis. *Proc. Natl. Acad. Sci. U.S.A. 100*, 2316–2321.
73. Kuzuyama, T., Noel, J. P., and Richard, S. B. (2005) Structural basis for the promiscuous biosynthetic prenylation of aromatic natural products. *Nature 435*, 983–987.